Articles

The Histone Gene Cell Cycle Regulator HiNF-P Is a Unique Zinc Finger Transcription Factor with a Novel Conserved Auxiliary DNA-Binding Motif†

Ricardo Medina, Timothy Buck, Sayyed K. Zaidi, Angela Miele-Chamberland, Jane B. Lian, Janet L. Stein, Andre J. van Wijnen, and Gary S. Stein*

Department of Cell Biology and Cancer Center, University of Massachusetts Medical School, Worcester, Massachusetts 01655

Received May 21, 2008; Revised Manuscript Received August 15, 2008

ABSTRACT: Accumulation of histone proteins is necessary for packaging of replicated DNA during the S phase of the cell cycle. Different mechanisms operate to regulate histone protein levels, and induction of human histone gene expression at the G1−S phase transition plays a critical role. The zinc finger HiNF-P and coactivator $p220^{NPAT}$ proteins are key regulators of histone gene expression. Here, we describe a novel HiNF-P-specific conserved region (PSCR) located within the C-terminus that is present in HiNF-P homologues of all metazoan species that have been examined. The PSCR motif is required for activation of histone H4 gene transcription and contributes to DNA binding of HiNF-P. Thus, the PSCR module represents an auxiliary DNA-binding determinant that plays a critical role in mediating histone gene expression during the cell cycle and defines HiNF-P as a unique cell cycle regulatory member of the zinc finger transcription factor family.

Histone protein synthesis must be finely coupled to DNA replication to accommodate the newly synthesized DNA during the S phase of the cell cycle (*1, 2*). Stringent control of histone gene expression is essential for normal cell proliferation, and abrogation of histone gene-related cell cycle mechanisms blocks cell growth (*3*). Multiple levels of regulation operate to ensure that histones are synthesized solely during the period of DNA synthesis. As a consequence of this orchestrated control, accumulation of histone mRNA is observed only when the protein is required. Transcriptional and posttranscriptional mechanisms regulate the level of histone mRNA during this period of the cell cycle. At the G1−/S phase transition, the extent of histone mRNA synthesis increases 3−5-fold (*4*−*7*). Posttranscriptional mechanisms include cell cycle regulation of the half-life of histone mRNAs (*8*) and S phase-specific endonucleolytic cleavage of the 3′-end of pre-mRNAs (*9, 10*).

The histone transcription factor HiNF-P is a critical component of a signaling pathway that controls expression of histone H4 genes during the S phase (*11*−*13*). HiNF-P exerts its regulatory function by physically interacting with and controlling the stability of $p220^{NPAT}$ (*14, 15*), a nuclear protein substrate of the cyclin E−CDK2 kinase complex that localizes to specific subnuclear foci (*16*−*18*). The HiNF-P−$p220^{NPAT}$ activation complex coordinately controls transcription of multiple histone H4 genes that are clustered in the human genome (*19*−*22*), and a similar $p220^{NPAT}$-dependent transcriptional mechanism has been proposed for histone H2B and H3 genes (*16, 17*). HiNF-P also recognizes non-histone targets, including genes that reinforce the cell cycle regulatory function of HiNF-P (*23*), as well as the HiNF-P gene itself (*24*). HiNF-P interacts with several proteins that have functions in transcription and/or RNA processing (*25*). These key findings together establish that HiNF-P is the end-point effector of a cyclin E−CDK2 signaling cascade that stimulates gene expression at the G1−S phase transition. Limited structure−function studies have been performed to date on this important cell cycle regulatory transcription factor (*14, 26*).

One major structural characteristic of HiNF-P is an N-terminal DNA-binding domain with a tandem array of nine zinc fingers of the C2H2 type (*14, 26*), in which two cysteines and two histidines coordinate a zinc ion to form a characteristic finger-like structure (*27*). The human genome encodes many zinc finger proteins that specifically control a large number of cellular regulatory pathways. Zinc finger proteins can be distinguished by the presence of auxiliary protein domains that are phylogenetically conserved and may support functional diversity. For example, conserved protein modules associated with zinc finger proteins include the poxvirus and zinc finger (POZ) domain, which is also known as the BTB (Broad-Complex, Tramtrack, and Bric-a-brac) domain (*28*), the Kruppel-associated box (KRAB) (*29*), and the SCAN domain (named after the four proteins initially found to contain this domain, SRE-ZBP, CTfin51, AW-1 [ZNF174], and Number 18 cDNA or ZnF20) (*30*).

The POZ/BTB domain is a repressor domain found in the promyelocytic leukemia zinc finger (PLZF) protein involved in embryonic development and hematopoiesis. The KRAB

† These studies were supported by NIH Grant GM032010.

* To whom correspondence should be addressed: Department of Cell Biology and Cancer Center, University of Massachusetts Medical School, 55 Lake Ave. N., Worcester, MA 01655. Telephone: (508) 856-5625. Fax: (508) 856-6800. E-mail: Gary.Stein@umassmed.edu.

10.1021/bi800961d CCC: $40.75
Published on Web 10/14/2008

domain is a transcriptional repressor found in transcription factors involved in hematopoietic cell development and differentiation. In contrast to POZ/BTB and KRAB domains, the SCAN domain is not associated with either transcriptional activation or repression. Recently, a new domain has been defined in zinc finger proteins, the SNAG (Snail/GFI-1) domain (*31*). This repressor domain is present in a variety of proto-oncogenic transcription factors and developmental regulators. Thus, zinc finger-associated modules typically support transcriptional repression and are usually located N-terminal to the zinc finger domain. In contrast, HiNF-P functions as an activator, and the only non-zinc finger region of the protein is located in the C-terminus and contributes to transactivation (*14*).

In this study, we describe a new 34-amino acid conserved region (PSCR)[1] in the C-terminus of HiNF-P, immediately adjacent to its zinc finger domain. The PSCR contributes to transcriptional activation of the histone H4 gene promoter through the cyclin E−CDK2−p220^{NPAT} pathway. We establish that the PSCR represents an auxiliary DNA-binding determinant and that a single amino acid (Y381) is critical for the DNA binding activity of HiNF-P. Our findings establish that HiNF-P is a unique member of the zinc finger transcription factor class. Its exquisite conservation throughout metazoan evolution is consistent with retention of a critical cell cycle regulatory role in mediating histone gene expression.

MATERIALS AND METHODS

Cell Culture. Human U-2 OS osteosarcoma cells were maintained in McCoy′s 5A medium (Invitrogen, Carlsbad, CA) supplemented with 10% fetal bovine serum (FBS), 2 mM L-glutamine, 100 units/mL penicillin G, and 100 μg/mL streptomycin. Human HeLa S3 cervical adenocarcinoma cells were maintained in Dulbecco′s modified Eagle′s medium (DMEM) (Invitrogen) supplemented with 10% FBS, 2 mM L-glutamine, 100 units/mL penicillin G, and 100 μg/mL streptomycin.

Mutagenesis of HiNF-P. Deletion mutants of HiNF-P were obtained by standard molecular procedures (*32*). For site-directed mutagenesis, mutant oligonucleotides were designed following the instructions provided with the QuickChange site-directed mutagenesis kit (Stratagene, La Jolla, CA). Reactions were carried out following the manufacturer′s instructions using a FLAG-tagged HiNF-P plasmid vector as a template. Two independent clones for each mutant construct were selected, full length sequenced, and analyzed. All oligonucleotides were gel purified by denaturing polyacrylamide gel electrophoresis. The oligonucleotides used were (in the 5′ to 3′ direction; only top strand shown) ΔPSCR (GTT CAA GTG GCC CCA ACC ACA AGA GG), ΔPSCR1 (GTT CAA GTG GCC CGA ACA TGA AGA TGG C), ΔPSCR2 (GCT GCA GCT GCT GAC ACA GCA ACT G), ΔPSCR3 (CTA CGA GAG TGT AGA GCA ACC ACA AGA GG), ΔPSCR4 (CCC GTT TTC GGT ACA AGG TTC GCT ACG), Y381A (GGC ATC CCC GTT TTC GGg caA AGG AAC ATG AAG ATG GCT), and Y381F (CAT CCC CGT TTT CGG TtC AAG GAA CAT GAA GAT GG). Underlined and lowercase letters represent positions for deletion and point mutations, respectively.

Reporter Gene Assays. Transient transfection of U-2 OS cells with FuGENE6 (Roche, Indianapolis, IN) was carried out in six-well plates seeded at a density of 0.13×10^6 cells per well. The next day, cells were transfected with 200 ng of either a luciferase construct with a minimal promoter sequence containing three HiNF-P binding sites (3× HiNF-P-Luc) or a luciferase construct spanning sites I and II of the histone H4/n gene promoter (H4/n-Luc). Expression vectors for epitope-tagged (FLAG) wild-type or mutant HiNF-P proteins (25 or 50 ng), p220^{NPAT} (200 ng), or the corresponding empty vectors (EV) were cotransfected. The total amount of DNA was kept the same in each transfection using the appropriate empty vectors. Cells were harvested 24 h after transfection, and cell lysates were measured for luciferase activity, which was normalized to Renilla (phRL-null) activity (dual-luciferase reporter assay system, Promega). Cell lysates (4%) were centrifuged at 16000*g* for 15 min at 4 °C and analyzed with a Western blot as described (see below).

Statistical Analysis. Unless otherwise noted, differences in transcriptional activity in reporter gene assays between the empty vector and expression vectors for wild-type or mutant HiNF-P and/or p220^{NPAT} were evaluated using general linear mixed models (*33*). Models were fit by restricted maximum likelihood estimation (*34*) using the SAS Proc Mixed procedure (*35*). In the presence of significant differences among means, pairwise comparisons were made using Tukey′s HSD test utilizing the estimated covariance matrix to account for correlated observations (*36*). The distributional characteristics of outcome measures were evaluated by applying the Kolmogorov−Smirnov Goodness of Fit Test for Normality (*37*) to residuals from fitted linear models and by inspection of frequency histograms of these residuals. Natural logarithms of outcomes were applied to better approximate normally distributed residuals. All computations were performed using SAS version 9.1.3 (*38*) and SPSS version 14 (SPSS Inc., Chicago, IL) statistical software packages. Results are presented as means ± standard errors transformed back into original units. Statistical significance exists when associated p values are less than 0.05. Differences with p values between 0.05 and 0.10 are described as "approaching significance".

Depletion of Endogenous HiNF-P by siRNA. For small interfering RNA (siRNA)-mediated knockdown of endogenous HiNF-P mRNA, U-2 OS cells were seeded in six-well plates at a density of 6.2×10^4 cells per well and transfected 24 h later with either *Silencer* Negative Control #1 siRNA (Ambion Inc., Austin, TX) or 3′UTR HiNF-P-specific double-stranded siRNA oligonucleotides (Ambion Inc.) at 25 nM with Oligofectamine according to the manufacturer′s instructions (Invitrogen, Carlsbad, CA). After siRNA transfection for 24 h, cells were treated as described for gene reporter assays.

Immunofluorescence Microscopy. U-2 OS cells were grown in six-well plates with coverslips (Fisher Scientific, Springfield, NJ), seeded at a density of 6×10^4 cells per well. After transfection for 24 h, cells were prepared for in situ immunofluorescence microscopy. Antibody staining was performed by incubating whole-cell preparations with mouse

[1] Abbreviations: PSCR, HiNF-P-specific conserved region; aa, amino acid; UTR, untranslated region; CDK, cyclin-dependent kinase; SDS, sodium dodecyl sulfate; DTT, dithiothreitol.

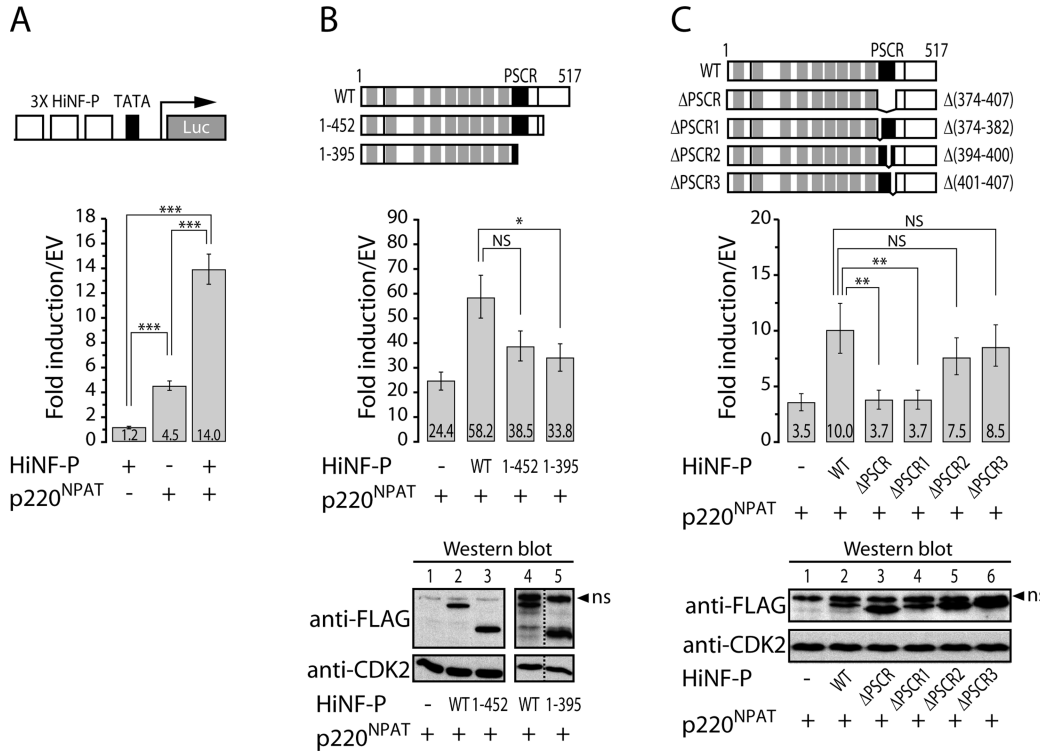

FIGURE 1: HiNF-P and p220^{NPAT} coactivation of a multimerized promoter requires the PSCR motif located at the C-terminus of HiNF-P. U-2 OS cells were transfected with a multimerized HiNF-P binding site fused to a minimal TATA box promoter−luciferase construct (3× HiNF-P−Luc) together with wild-type or mutant HiNF-P and p220^{NPAT} proteins. (A) Expression of p220^{NPAT} alone results in a 4.5-fold activation, and coexpression of HiNF-P and p220^{NPAT} elevates the promoter activity by 14.0-fold. (B) Progressive external deletion of the C-terminal region of HiNF-P abolishes the coactivation of promoter activity induced by cotransfection of wild-type HiNF-P and p220^{NPAT}. Both deletion mutants, aa 1−452 and aa 1−395, show basal transcriptional levels similar to that achieved by transfection with p220^{NPAT} alone, although only mutant 1−395 attains statistical significance. The top portion shows a diagram of wild-type (WT) and HiNF-P mutant proteins. Depicted are the zinc finger motif (gray boxes), the HiNF-P-specific conserved region (PSCR; black box), and two acidic regions (black lines). The bottom panel shows similar protein levels for wild-type (WT) and external deletion mutant HiNF-P proteins from the indicated luciferase samples detected by Western blot analysis using FLAG antibody (CDK2 is shown as loading control; ns, nonspecific). (C) Internal deletion of the PSCR motif (ΔPSCR; aa 374−407) as well as deletion of aa 374−382 (ΔPSCR1), but neither aa 394−400 (ΔPSCR2) nor aa 401−407 (ΔPSCR3) of HiNF-P, abolishes transcriptional coactivation of the HiNF-P responsive promoter. The top portion shows a diagram of wild-type (WT) and HiNF-P mutant proteins. The bottom panel shows similar protein levels for wild-type (WT) and internal deletion mutant HiNF-P proteins from the indicated luciferase samples detected by Western blot analysis using FLAG antibody (CDK2 is shown as loading control; ns, nonspecific). Results are presented as means ± the standard error. NS, not significant. †, $0.05 < p < 0.1$; *, $p < 0.05$; **, $p < 0.01$; ***, $p < 0.001$.

monoclonal anti-FLAG clone M2 (Sigma, St. Louis, MO) at a 1:5000 dilution for 1 h at 37 °C. The secondary antibody (Alexa 568 goat anti-mouse IgG; Molecular Probes, Eugene, OR) was used at a 1:800 dilution. Immunostaining of cell preparations was captured by an epifluorescence microscope (Zeiss Axioplan II) equipped with a charge-coupled device camera. Digital images were acquired as grayscale and transformed to eight-bit images using MetaMorph (Molecular Devices, Downingtown, PA). The images were pseudocolored to green using the channel mixer tool of Adobe Photoshop. All images were processed in the same manner.

In Vitro-Coupled Transcription and Translation and Nuclear Protein Preparation. In vitro-transcribed and -translated (IVTT) protein was produced by the TNT Coupled Reticulocyte Lysate System (Promega, Madison, WI). For nuclear extract preparation, HeLa cells were seeded at a density of 5×10^5 in 100 mm plates and 24 h later transfected with plasmid DNA (4 μg per plate) using FuGENE6 following the manufacturer's instructions. After transfection for 24 h, cells were collected and centrifuged at 1000*g* for 5 min at 4 °C. All subsequent procedures were conducted at 4 °C. The supernatant was removed, and the cell pellet was resuspended in 400 μL of ice-cold lysis buffer [10 mM Tris-HCl (pH 7.4), 3 mM $MgCl_2$, 10 mM NaCl, and 0.5% NP-40] by gentle pipet mixing. Cells were incubated on ice for 10 min and then centrifugated at 16000*g* for 30 s. After the supernatant was removed, the pellet was resuspended in 400 μL of ice-cold buffer [10 mM HEPES (pH 7.9), 1.5 mM $MgCl_2$, and 10 mM KCl]. After centrifugation at 4500*g* for 1 min, the supernatant was carefully removed and the nuclear pellet was resuspended in 100 μL of ice-cold extraction buffer [20 mM HEPES (pH 7.9), 1.5 mM $MgCl_2$, 420 mM KCl, 0.2 mM EDTA, and 20% glycerol]. Nuclei were incubated with constant agitation at 4 °C for 45 min. Nuclear extracts were recovered by centrifugation at 16000*g* for 5 min, snap-frozen in liquid nitrogen, and kept at −80 °C until they were used. The protein content was quantified by a Bradford assay (Pierce, Rockford, IL).

Western Blotting Analysis. Nuclear extracts or IVTT-produced proteins were loaded onto 10% sodium dodecyl sulfate (SDS)−polyacrylamide gels and transferred to a polyvinylidene fluoride (PVDF) Immobilon-P membrane (Millipore, Billerica, MA) for 30 min at 10 V in a semidry transfer apparatus (model HEP-1, Owl Separation Systems, Portsmouth, NH). Immunodetection was performed using an

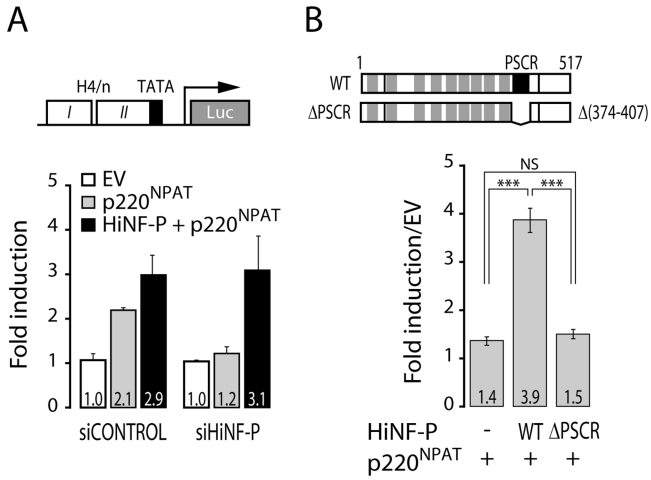

FIGURE 2: PSCR motif of HiNF-P is required for the coactivation of the wild-type histone H4 gene promoter. U-2 OS cells were transfected with the wild-type histone H4/n gene promoter−luciferase reporter construct (H4/n−Luc) together with wild-type or mutant HiNF-P and p220^{NPAT} proteins. (A) Depletion of endogenous HiNF-P by siRNA abolishes p220^{NPAT} coactivation. Cells were transfected with control siRNA (siCONTROL) or 3′-UTR-specific HiNF-P siRNA (siHiNF-P) oligonucleotides for 24 h followed by transfection with a H4/n−Luc construct together with empty vector or expression vectors for HiNF-P and p220^{NPAT} for 24 h. Transfection with p220^{NPAT} alone produces a 2.1-fold activation of the reporter construct in siCONTROL-treated cells, but this level returns to basal transcriptional activity levels when cells are depleted of HiNF-P (siHiNF-P). Transfection of exogenous HiNF-P together with p220^{NPAT} in HiNF-P-depleted cells (siHiNF-P) re-establishes the coactivation observed in control-treated cells (siCONTROL). Results are presented as means ± the standard deviation. (B) HiNF-P and p220^{NPAT} coactivation of the wild-type histone H4 gene promoter requires the PSCR motif of HiNF-P. U-2 OS cells were treated with a 3′-UTR-specific HiNF-P siRNA oligonucleotide (25 nM) for 24 h as described above and transfected with a H4/n−Luc construct together with expression vectors for wild-type HiNF-P (WT), mutant ΔPSCR HiNF-P, and p220^{NPAT} proteins for 24 h. Transcriptional basal levels are observed in HiNF-P-depleted U-2 OS cells when p220^{NPAT} is transfected alone. Transfection of exogenous wild-type HiNF-P together with p220^{NPAT} produces a 3.9-fold coactivation; however, transfection of mutant ΔPSCR together with p220^{NPAT} abolishes this coactivation. Results are presented as means ± the standard error. NS, not significant. †, $0.05 < p < 0.1$; *, $p < 0.05$; **, $p < 0.01$; ***, $p < 0.001$. The top panel shows a diagram of wild-type (WT) and mutant ΔPSCR HiNF-P proteins; deleted amino acids are indicated at the right (for further details, see Figure 1B).

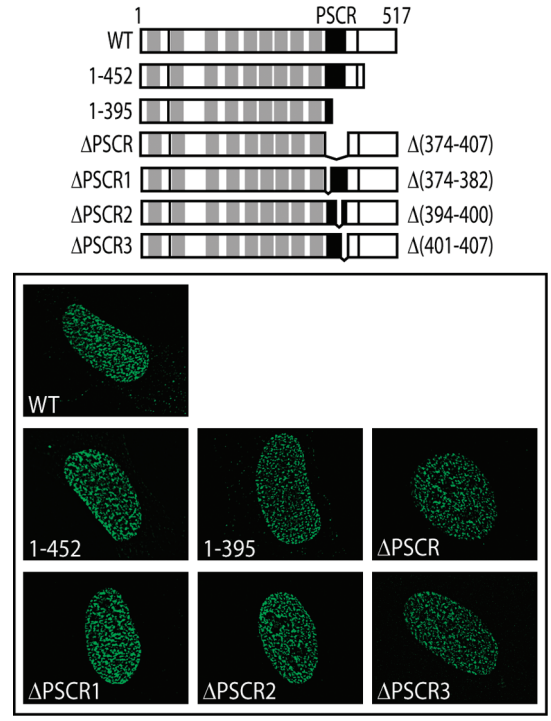

FIGURE 3: Subcellular localization of wild-type and mutant HiNF-P proteins. Human U-2 OS cells were grown on coverslips, transfected with FLAG-tagged proteins, and analyzed by in situ immunofluorescence microscopy. Wild-type and mutant HiNF-P proteins (see diagram) were detected using a mouse monoclonal FLAG (M2) antibody. Wild-type as well as external (aa 1−452 and aa 1−395) and internal (ΔPSCR, ΔPSCR1, ΔPSCR2, and ΔPSCR3) deletion HiNF-P proteins exhibit characteristic nuclear staining.

appropriate dilution of specific antibodies with the Western Lightning Chemiluminescence Reagent Plus assay (Perkin-Elmer Life Sciences, Waltham, MA). The following dilutions of primary antibodies were used: rabbit polyclonal CDK2 at 1:5000 (M-2, sc163; Santa Cruz Biotechnology Inc., Santa Cruz, CA), mouse monoclonal FLAG at 1:5000 (M2, Sigma), and rabbit polyclonal HiNF-P at 1:2000.

Electrophoretic Mobility Shift Assay. Binding of wild-type or mutant HiNF-P proteins to a specific double-stranded oligonucleotide was assessed either with nuclear extracts overexpressing FLAG tag or with IVTT-produced proteins. In vitro, DNA binding reactions were performed by combining 2−5 μg of nuclear extracts or 1−8 μL of IVTT-produced protein in a total volume of 9 μL of protein buffer [final concentrations of 9 mM HEPES (pH 7.5), 0.09 mM EDTA (pH 8.0), 50 mM KCl, 10% glycerol, 1× Complete protease inhibitor (Roche, Indianapolis, IN), 1 mM NaF, and 1 mM Na_3VO_4] with 10 μL of a DNA mixture containing 10−20 fmol of labeled, double-stranded oligonucleotide in DNA buffer (final concentrations of 0.1 μg/μL salmon sperm DNA, 1 mM DTT, 0.5 mM $MgCl_2$, and 0.1 mM $ZnCl_2$). Where indicated, unlabeled oligonucleotide competitor (in 1 μL) was added in a 100-fold molar excess. Mixtures were incubated for 20 min at room temperature, and the protein−DNA complexes were then separated in 4% (40:1) native polyacrylamide gels using 1× TBE as the running buffer at 4 °C. Gels were dried and exposed to BioMax XAR or MR (Kodak, New Haven, CT) films at −80 °C. The following oligonucleotides were used (in the 5′ to 3′ direction): an optimized HiNF-P binding site based on its recognition sequence in site II of the H4/n gene (CTT CAG GTT TTC AAT CTG GTC CGA TAC T), HiNF-P mutant (CTT CAG GTT TTC AAT CTT CTA CGA TAC T) (mutated nucleotides underlined), and nonspecific competitor (ATT CGA TCG GGG CGG GGC GAG C).

Sequence Alignment and Three-Dimensional Modeling. Multiple-sequence alignment to obtain structure−function information about PSCR motifs among HiNF-P homologues was done using ClustalW and GeneDoc (*39*). Three-dimensional modeling of the PSCR motif was performed using 3D-Phyre (*40, 41*).

RESULTS

A Conserved C-Terminal Domain in HiNF-P Contributes to Histone H4 Gene Transcriptional Activation by the HiNF-P−p220^{NPAT} Complex. The histone H4 transcription factor HiNF-P has an N-terminal domain containing nine zinc fingers and a C-terminal region with unknown function.

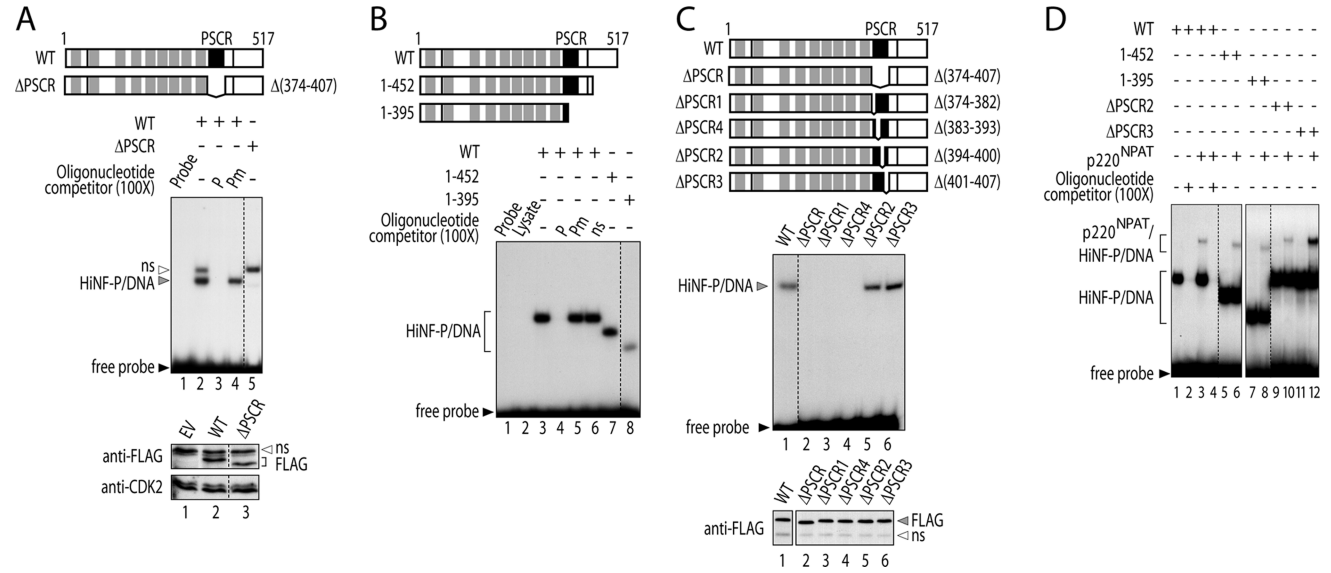

FIGURE 4: PSCR domain of HiNF-P is an auxiliary DNA-binding determinant. Protein binding to DNA was tested using a radioactively labeled optimized HiNF-P binding site oligonucleotide by an electrophoretic mobility shift assay (EMSA). (A) Binding of wild-type or ΔPSCR mutant HiNF-P proteins overexpressed in HeLa cells was tested by an EMSA using nuclear extracts. Wild-type HiNF-P forms a distinct protein−DNA complex (lane 2; gray arrowhead), and a nonspecific band (ns; empty arrowhead) is also observed; competition experiments with specific wild-type (P; lane 3) or mutant (Pm; lane 4) unlabeled oligonucleotides were performed with a 100-fold molar excess. The ΔPSCR HiNF-P mutant lacks the ability to bind to the HiNF-P binding site (lane 5). The subcellular localization and equivalence of expression levels for wild-type (lane 2) and ΔPSCR mutant (lane 3) HiNF-P proteins were confirmed by Western blot (bottom panel; CDK2 is shown as a loading control) using a FLAG antibody (ns, nonspecific). (B) EMSA with recombinant wild-type and mutant HiNF-P proteins produced by a coupled in vitro-transcribed and -translated (IVTT) system. Recombinant wild-type HiNF-P binds to its recognition binding site to form a single protein−DNA complex band (lane 3). Specificity was assessed by competition with specific wild-type (P; lane 4), mutant (Pm; lane 5), or nonspecific (ns; lane 6) unlabeled oligonucleotides at a 100-fold molar excess. The external deletion mutants 1−452 (lane 7) and 1−395 (lane 8) are both capable of binding to a HiNF-P element, although the 1−395 mutant exhibits decreased binding activity (compare lane 8 with lane 3). (C) EMSA with IVTT-produced wild-type (lane 1) and ΔPSCR deletion (lanes 2−6) HiNF-P proteins. The recombinant mutant proteins ΔPSCR (lane 2), ΔPSCR1 (lane 3), and ΔPSCR4 (lane 4) do not bind to the HiNF-P-binding motif, while mutants ΔPSCR2 (lane 5) and ΔPSCR3 (lane 6) remain competent for binding. Recombinant wild-type and mutant proteins were all produced at comparable levels, as demonstrated by Western blot analysis using a FLAG antibody (bottom panel; ns, nonspecific). (D) EMSAs with IVTT-produced $p220^{NPAT}$ together with wild-type (lanes 1−4) and mutant HiNF-P proteins (lanes 5−12). We tested external 1−452 (lanes 5 and 6) and 1−395 (lanes 7 and 8) and internal ΔPSCR2 (lanes 9 and 10) and ΔPSCR3 (lanes 11 and 12) HiNF-P deletion proteins. Formation of a ternary $p220^{NPAT}$−HiNF-P−DNA complex was assayed by combining HiNF-P proteins with (lanes 3, 4, 6, 8, 10, and 12) or without (lanes 1, 2, 5, 7, 9, and 11) an N-terminal segment of $p220^{NPAT}$. Specificity of complex formation was assessed by competition with a 100-fold excess of unlabeled HiNF-P DNA oligonucleotide (lanes 2 and 4). Depicted on the left are the positions of the HiNF-P−DNA and $p220^{NPAT}$−HiNF-P−DNA complexes. Gels were overexposed to enhance visualization of the ternary complex.

Several zinc finger transcription factors have conserved motifs outside the zinc finger domain (e.g., POZ/BTB, KRAB, SCAN, and SNAG domains) (*31, 42*). Similarly, sequence alignment analysis reveals that the transcription factor HiNF-P possesses an evolutionarily conserved sequence of 34 amino acids in its C-terminal region [HiNF-P-specific conserved region (PSCR), aa 374−407] (see Figure 6). To address whether this conserved region has a role in HiNF-P−$p220^{NPAT}$ complex-dependent activation of histone H4 gene transcription, we constructed a series of HiNF-P mutants with external and internal deletions in the C-terminus. Wild-type HiNF-P and $p220^{NPAT}$ synergize to produce a 14-fold induction of a luciferase reporter controlled by a multimerized HiNF-P recognition site in U-2 OS cells, while transfection of $p220^{NPAT}$ alone produces an only 4.5-fold induction (Figure 1A), consistent with previous findings (*14*). Deletion of the C-terminus of HiNF-P to either amino acid 452 or 395 in each case abolishes coactivation of the HiNF-P responsive promoter in U-2 OS cells in the presence of $p220^{NPAT}$ (Figure 1B). These results suggest that the C-terminus of HiNF-P between amino acids 452 and 517 contributes to transcriptional activation. Strikingly, internal deletion of the PSCR completely abolishes HiNF-P−$p220^{NPAT}$ complex coactivation of the multimerized histone H4 promoter (Figure 1C). To further characterize the PSCR, we generated three additional internal deletions within the PSCR. Deletion of aa 374−382 (ΔPSCR1), but neither aa 394−400 (ΔPSCR2) nor aa 401−407 (ΔPSCR3) of HiNF-P, abrogates transcriptional coactivation of the HiNF-P responsive promoter (Figure 1C). Thus, these results establish that the PSCR of HiNF-P is required for synergistic activation of histone H4 gene transcription together with $p220^{NPAT}$.

We tested whether the PSCR is required for transcriptional activation of the native histone H4 gene promoter by the HiNF-P−$p220^{NPAT}$ complex (Figure 2). To increase the sensitivity of reporter gene expression to exogenous wild-type and mutant HiNF-P, we depleted endogenous HiNF-P levels using a siRNA approach. We selected a HiNF-P siRNA that specifically targets the 3′-UTR of the native HiNF-P mRNA but does not affect exogenously expressed HiNF-P because our expression constructs lack these 3′-UTR sequences. The HiNF-P siRNA oligonucleotide treatment was initiated 24 h prior to transfections with plasmid vectors. The histone H4 gene promoter is only activated by $p220^{NPAT}$ when HiNF-P levels are not depleted by siRNA (Figure 2A), corroborating our previous results (*14*). Exogenous expression of wild-type HiNF-P restores $p220^{NPAT}$ activation

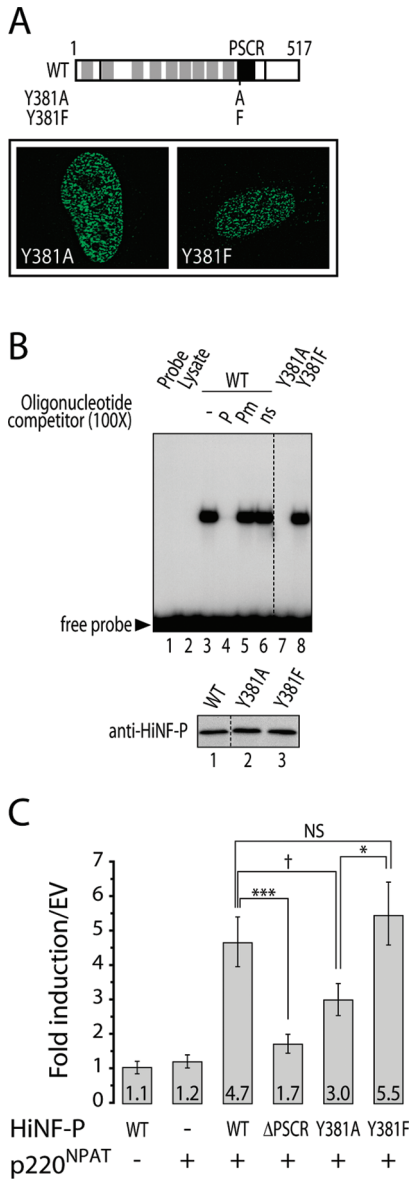

FIGURE 5: Mutation of tyrosine 381 within the PSCR motif of HiNF-P abolishes its DNA binding activity. (A) Nuclear localization of point mutants Y381A and Y381F of HiNF-P was established by immunofluorescence in human U-2 OS cells as described in the legend of Figure 3. The top portion shows a diagram of HiNF-P and the position of the mutated tyrosine within the PSCR (for further details, see Figures 1B and 6). (B) EMSA with recombinant wild-type and point mutant HiNF-P proteins produced by coupled IVTT. Recombinant wild-type HiNF-P binds to its recognition element to form a single protein−DNA complex band (lane 3). Specificity was assessed by competition with specific wild-type (P; lane 4), mutant (Pm; lane 5), or nonspecific (ns; lane 6) unlabeled oligonucleotides at a 100-fold molar excess. Mutation of tyrosine 381 to alanine (lane 7) but not to phenylalanine (lane 8) abolishes binding of HiNF-P to its cognate binding site. Recombinant wild-type (lane 1) and point mutant (lanes 2 and 3) proteins were all produced at comparable levels as demonstrated by Western blot analysis using FLAG antibodies (bottom panel). (C) HiNF-P-depleted U-2 OS cells were transfected with a H4/n−Luc construct together with expression vectors for wild-type HiNF-P (WT), mutant Y381A or Y381F, and p220^{NPAT} for 24 h. Basal levels are observed when p220^{NPAT} is transfected alone. Transfection of exogenous wild-type HiNF-P together with p220^{NPAT} produces a 4.7-fold coactivation; however, the cotransfection of mutant ΔPSCR and p220^{NPAT} is incapable of coactivation. The Y381A mutation but not the Y381F mutation decreases the transactivation potential of HiNF-P and p220^{NPAT} on the histone H4 promoter. Results are presented as means ± the standard error. NS, not significant. †, $0.05 < p < 0.1$; *, $p < 0.05$; **, $p < 0.01$; and ***, $p < 0.001$.

(Figure 2A,B), while the HiNF-P mutant ΔPSCR (aa 374−407) does not (Figure 2B). Hence, the PSCR is required for the transmission of signals from the cyclin E−CDK2−p220^{NPAT} pathway that stimulate transcription of the cell cycle-regulated native histone H4 gene promoter.

The PSCR Motif Represents an Auxiliary DNA-Binding Determinant. To ensure that the exogenous wild-type and mutant HiNF-P proteins are properly directed to the nucleus, we performed immunofluorescence (IF) microscopy and electrophoretic mobility shift assays (EMSAs) with nuclear lysates. Wild-type HiNF-P as well as external (aa 1−452 and aa 1−395) and internal deletions encompassing the PSCR sequences (ΔPSCR, ΔPSCR1, ΔPSCR2, and ΔPSCR3) are all localized to the nucleus (Figure 3). This finding demonstrates that loss of transcriptional coactivation upon deletion of the PSCR motif of HiNF-P is not due to subcellular mislocalization but reinforces the idea that this conserved region is important for HiNF-P function. Our data also indicate that a nuclear localization signal is present in the N-terminal zinc finger region of HiNF-P between amino acids 1 and 395.

Wild-type HiNF-P forms a characteristic HiNF-P−DNA complex in EMSAs that is effectively competed by an unlabeled wild-type oligonucleotide but not by the corresponding mutant oligonucleotide (Figure 4A, lanes 2−4). When we examined the levels of HiNF-P mutants in nuclear lysates using EMSAs, we did not observe the expected protein−DNA complex for the ΔPSCR mutant (Figure 4A, lane 5). However, IF data (Figure 3) and Western blot data (Figure 4A, bottom panel) clearly indicate the presence of this mutant protein in the nucleus.

To examine whether this protein may have lost the ability to bind the HiNF-P recognition motif, we performed EMSAs with recombinant HiNF-P proteins that where produced by coupled in vitro transcription and translation (Figure 4B,C). Recombinant wild-type and mutant proteins were all produced at the same levels, as demonstrated by Western blot analysis (Figure 4C, bottom panel). The external deletion mutants 1−452 and 1−395 are both capable of sequence-specific binding to the histone H4 gene promoter in vitro; however, the 1−395 mutant exhibits slightly weakened binding (Figure 4B, lane 8). Strikingly, the recombinant ΔPSCR mutant protein does not bind to the HiNF-P probe (Figure 4C, lane 2). Therefore, we also monitored binding of four additional internal deletion mutants of the PSCR region. Removal of aa 394−400 or aa 401−407 (i.e., mutants ΔPSCR2 and ΔPSCR3) does not affect DNA binding (Figure 4C, lanes 5 and 6), but deletion of either aa 374−382 or aa 383−393 (i.e., mutants ΔPSCR1 and ΔPSCR4) of HiNF-P abolishes DNA binding activity (Figure 4C, lanes 3 and 4). The loss of binding of ΔPSCR4 (Figure 4C, lane 4) is consistent with the weakened protein−DNA interaction observed for the 1−395 deletion, which is apparently truncated near amino acids of HiNF-P required for DNA binding (see lane 8 of Figure 4B). Taken together, these findings establish that the N-terminal segment (aa 374−393) of the PSCR motif is required for DNA binding of HiNF-P and thus represents an auxiliary DNA-binding determinant.

To test whether HiNF-P mutants still retain their ability to interact with p220^{NPAT}, we performed EMSAs to detect the p220^{NPAT}−HiNF-P−DNA ternary complex (Figure 4D). We used recombinant HiNF-P proteins and a truncated

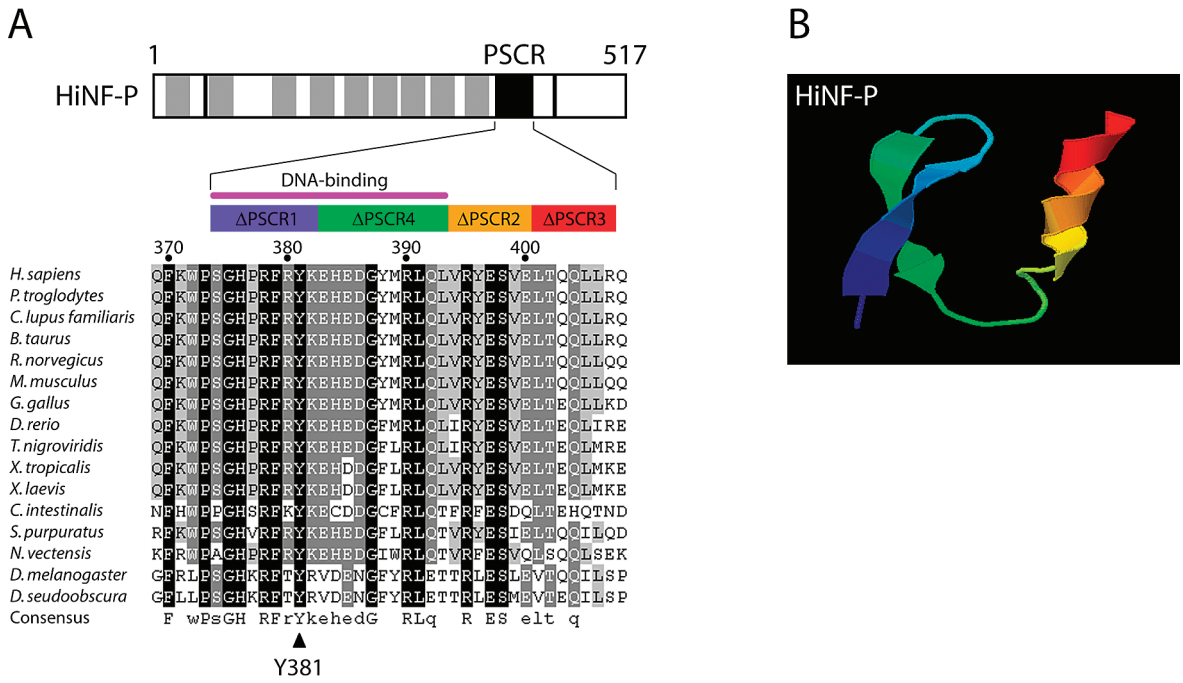

FIGURE 6: PSCR motif of HiNF-P is conserved throughout evolution. (A) Multiple-sequence alignment of the PSCR region of human HiNF-P with the corresponding amino acid residues from different metazoan species. Alignments were performed with ClustalW and GeneDoc. Black, dark gray, and light gray shades represent 100, 80−95, and 60−75% conservation, respectively. Conserved residues within a putative consensus sequence of the PSCR are shown below the alignment. The purple line above the diagram shows the part of the PSCR required for DNA binding, and the filled arrowhead at the bottom shows a residue critical for the DNA binding activity of HiNF-P. (B) Molecular modeling of the PSCR of human HiNF-P using 3D-Phyre (*40, 41*). Colored regions correspond to the PSCR segments in the diagram in panel A.

p220^{NPAT} protein corresponding to aa 1−499 that we have previously shown interacts functionally with HiNF-P (*14*). In the presence of p220^{NPAT}, full-length HiNF-P forms a ternary complex that is detected by an EMSA as a band of reduced mobility (Figure 4D, lane 3) and is specifically competed by HiNF-P oligonucleotide (Figure 4D, lane 4). We monitored the interaction of all four HiNF-P deletion mutants which still retain their ability to bind DNA. External deletion mutants 1−452 and 1−395 as well as internal deletions ΔPSCR2 and ΔPSCR3 (aa 394−400 and aa 401−407, respectively) still form a ternary complex with p220^{NPAT}. These results suggest that the C-terminal portion of HiNF-P beyond aa 395 is not required for p220^{NPAT} interaction.

A Single-Point Mutation within the PSCR Motif Abolishes DNA Binding Activity of HiNF-P. The N-terminal segment of the PSCR is composed of 34 conserved amino acids (SGHPR FRYKE HEDGY MRLQL VRYES VELTQ QLLR). We generated four separate alanine substitutions (S374A, Y381A, K382A, and Y388A) that were tested for DNA binding activity in EMSAs as recombinant proteins or in nuclear extracts (Figure 5 and data not shown). All proteins produced by IVTT or in transient transfections were expressed at similar levels by Western blot analysis (Figure 5B, bottom panel and data not shown). The HiNF-P point mutants are present in the nucleus as demonstrated by immunofluorescence microscopy (Figure 5A and data not shown). Mutation S374A, K382A, or Y388A does not significantly affect DNA binding (data not shown). However, alanine mutation of Y381 abolishes the interaction of HiNF-P with its cognate site (Figure 5B, lane 7). In contrast, mutation of Y381 to phenylalanine (mutant Y381F) does not abolish the DNA binding activity of HiNF-P (Figure 5B, lane 8). The differences in DNA binding activity of the Y381A and Y381F point mutants are directly reflected by differences in their transactivation potential on the histone H4 gene promoter (Figure 5C). Our data establish that tyrosine 381 is critical for HiNF-P DNA binding and corroborate the conclusion that the PSCR motif contributes to the ability of HiNF-P to recognize its cognate cell cycle regulatory element. Three-dimensional modeling of the PSCR motif suggests that this segment of HiNF-P has the potential to form a β-hairpin−α-helix structure that is perhaps analogous to the zinc-stabilized β-strand−α-helix structure typically observed in zinc finger modules (Figure 6).

DISCUSSION

Previous studies revealed that the human histone H4 transcription factor HiNF-P contains nine N-terminal zinc fingers and that its C-terminus contributes to transcriptional activation of histone H4 genes (*14*). Here, we show that HiNF-P contains a highly conserved 34-amino acid region (PSCR) within the C-terminus that represents an auxiliary DNA-binding determinant. Experimental data and molecular modeling of the PSCR suggest that there are two distinct peptides (aa 374−393 and aa 394−407). While the 394−407 peptide is dispensable for DNA binding, the 374−393 peptide is required and a point mutation of a conserved tyrosine residue (Y381) is sufficient to abolish sequence-specific binding to and activation of the histone H4 gene promoter.

The identification of the PSCR domain defines HiNF-P as a unique member of the zinc finger transcription factor family that is distinct from four major subgroups of zinc finger proteins that have been described in other studies.

Many zinc finger proteins contain an auxiliary module that is typically located in the N-terminus of the protein, including the POZ/BTB (*28*), KRAB (*29*), SCAN (*30*), and SNAG domains (*31*). Unlike the PSCR domain, the POZ/BTB, KRAB, and SNAG modules have all been characterized as repressor domains, while the SCAN domain contributes to transcriptional control through dimerization. In contrast to these motifs, which are all involved in protein−protein interactions, one important function of the PSCR region is to facilitate DNA binding of HiNF-P to support its critical role in cell cycle-dependent activation of the histone H4 gene promoter.

Histones are encoded by a multigene family and are essential for chromatin structure and cell viability in species from yeast to humans. While the zinc finger region of HiNF-P is similar to a large number of mammalian transcription factors, the PSCR is not present in any other protein encoded by the human genome. This observation indicates that HiNF-P is a singular member of the zinc finger protein family that is at least in part dedicated to histone gene expression. Although there is no paralog for HiNF-P in the human genome, the PSCR is highly conserved in putative homologues of HiNF-P in all metazoan species for which sequence information is available. The conservation of the PSCR motif suggests that the regulatory function of HiNF-P originated early during evolution of multicellular species.

In conclusion, our data demonstrate that the C-terminus of HiNF-P contains a novel protein segment that is critical for the cell cycle regulatory function of HiNF-P in activation of histone gene expression. The unique nature of this protein segment may permit the development of inhibitory molecules that will block HiNF-P function as a potential strategy for intervening in deregulated proliferation of cancer cells.

ACKNOWLEDGMENT

We thank Judy Rask for expert assistance in the preparation of the manuscript and Stephen Baker for expert advice with statistical analysis. We also thank the members of our research group and especially Rong-Lin Xie and Margaretha van der Deen for stimulating discussions.

REFERENCES

1. Stein, G. S., Stein, J. L., van Wijnen, A. J., and Lian, J. B. (1992) Regulation of histone gene expression. *Curr. Opin. Cell Biol. 4*, 166–173.
2. Stein, G. S., van Wijnen, A. J., Stein, J. L., Lian, J. B., Montecino, M., Zaidi, S. K., and Braastad, C. (2006) An architectural perspective of cell-cycle control at the G1/S phase cell-cycle transition. *J. Cell. Physiol. 209*, 706–710.
3. Ye, X., Wei, Y., Nalepa, G., and Harper, J. W. (2003) The cyclin E/Cdk2 substrate p220(NPAT) is required for S-phase entry, histone gene expression, and Cajal body maintenance in human somatic cells. *Mol. Cell. Biol. 23*, 8586–8600.
4. Plumb, M., Stein, J., and Stein, G. (1983) Coordinate regulation of multiple histone mRNAs during the cell cycle in HeLa cells. *Nucleic Acids Res. 11*, 2391–2410.
5. Baumbach, L. L., Stein, G. S., and Stein, J. L. (1987) Regulation of human histone gene expression: Transcriptional and posttranscriptional control in the coupling of histone messenger RNA stability with DNA replication. *Biochemistry 26*, 6178–6187.
6. Heintz, N., Sive, H. L., and Roeder, R. G. (1983) Regulation of human histone gene expression: Kinetics of accumulation and changes in the rate of synthesis and in the half-lives of individual histone mRNAs during the HeLa cell cycle. *Mol. Cell. Biol. 3*, 539–550.
7. Harris, M. E., Bohni, R., Schneiderman, M. H., Ramamurthy, L., Schumperli, D., and Marzluff, W. F. (1991) Regulation of histone mRNA in the unperturbed cell cycle: Evidence suggesting control at two posttranscriptional steps. *Mol. Cell. Biol. 11*, 2416–2424.
8. Morris, T. D., Weber, L. A., Hickey, E., Stein, G. S., and Stein, J. L. (1991) Changes in the stability of a human H3 histone mRNA during the HeLa cell cycle. *Mol. Cell. Biol. 11*, 544–553.
9. Dominski, Z., and Marzluff, W. F. (1999) Formation of the 3′ end of histone mRNA. *Gene 239*, 1–14.
10. Dominski, Z., and Marzluff, W. F. (2007) Formation of the 3′ end of histone mRNA: Getting closer to the end. *Gene 396*, 373–390.
11. van Wijnen, A. J., van den Ent, F. M., Lian, J. B., Stein, J. L., and Stein, G. S. (1992) Overlapping and CpG methylation-sensitive protein-DNA interactions at the histone H4 transcriptional cell cycle domain: Distinctions between two human H4 gene promoters. *Mol. Cell. Biol. 12*, 3273–3287.
12. Mitra, P., Xie, R. L., Medina, R., Hovhannisyan, H., Zaidi, S. K., Wei, Y., Harper, J. W., Stein, J. L., van Wijnen, A. J., and Stein, G. S. (2003) Identification of HiNF-P, a key activator of cell cycle controlled histone H4 genes at the onset of S phase. *Mol. Cell. Biol. 23*, 8110–8123.
13. Mitra, P., Xie, R., Harper, J. W., Stein, J. L., Stein, G. S., and van Wijnen, A. J. (2007) HiNF-P is a bifunctional regulator of cell cycle controlled histone H4 gene transcription. *J. Cell. Biochem. 101*, 181–191.
14. Miele, A., Braastad, C. D., Holmes, W. F., Mitra, P., Medina, R., Xie, R., Zaidi, S. K., Ye, X., Wei, Y., Harper, J. W., van Wijnen, A. J., Stein, J. L., and Stein, G. S. (2005) HiNF-P directly links the cyclin E/CDK1/p220^{NPAT} pathway to histone H4 gene regulation at the G1/S phase cell cycle transition. *Mol. Cell. Biol. 25*, 6140–6153.
15. Medina, R., van Wijnen, A. J., Stein, G. S., and Stein, J. L. (2006) The histone gene transcription factor HiNF-P stabilizes its cell cycle regulatory co-activator p220^{NPAT}. *Biochemistry 45*, 15915–15920.
16. Zhao, J., Kennedy, B. K., Lawrence, B. D., Barbie, D. A., Matera, A. G., Fletcher, J. A., and Harlow, E. (2000) NPAT links cyclin E-Cdk2 to the regulation of replication-dependent histone gene transcription. *Genes Dev. 14*, 2283–2297.
17. Ma, T., Van Tine, B. A., Wei, Y., Garrett, M. D., Nelson, D., Adams, P. D., Wang, J., Qin, J., Chow, L. T., and Harper, J. W. (2000) Cell cycle-regulated phosphorylation of p220(NPAT) by cyclin E/Cdk2 in Cajal bodies promotes histone gene transcription. *Genes Dev. 14*, 2298–2313.
18. Ghule, P. N., Becker, K. A., Harper, J. W., Lian, J. B., Stein, J. L., van Wijnen, A. J., and Stein, G. S. (2007) Cell cycle dependent phosphorylation and subnuclear organization of the histone gene regulator p220^{NPAT} in human embryonic stem cells. *J. Cell. Physiol. 213*, 9–17.
19. Holmes, W. F., Braastad, C. D., Mitra, P., Hampe, C., Doenecke, D., Albig, W., Stein, J. L., van Wijnen, A. J., and Stein, G. S. (2005) Coordinate control and selective expression of the full complement of replication-dependent histone H4 genes in normal and cancer cells. *J. Biol. Chem. 280*, 37400–37407.
20. Braastad, C. D., Hovhannisyan, H., van Wijnen, A. J., Stein, J. L., and Stein, G. S. (2004) Functional characterization of a human histone gene cluster duplication. *Gene 342*, 35–40.
21. Becker, K. A., Stein, J. L., Lian, J. B., van Wijnen, A. J., and Stein, G. S. (2007) Establishment of histone gene regulation and cell cycle checkpoint control in human embryonic stem cells. *J. Cell. Physiol. 210*, 517–526.
22. Doenecke, D., Albig, W., Bode, C., Drabent, B., Franke, K., Gavenis, K., and Witt, O. (1997) Histones: Genetic diversity and tissue-specific gene expression. *Histochem. Cell Biol. 107*, 1–10.
23. Medina, R., van der Deen, M., Miele-Chamberland, A., Xie, R. L., van Wijnen, A. J., Stein, J. L., and Stein, G. S. (2007) The HiNF-P/p220^{NPAT} cell cycle signaling pathway controls non-histone target genes. *Cancer Res. 67*, 10334–10342.
24. Xie, R. L., Liu, L., Mitra, P., Stein, J. L., van Wijnen, A. J., and Stein, G. S. (2007) Transcriptional activation of the histone nuclear factor P (HiNF-P) gene by HiNF-P and its cyclin E/CDK2 responsive co-factor p220(NPAT) defines a novel autoregulatory loop at the G1/S phase transition. *Gene 402*, 94–102.
25. Miele, A., Medina, R., van Wijnen, A. J., Stein, G. S., and Stein, J. L. (2007) The interactome of the histone gene regulatory factor HiNF-P suggests novel cell cycle related roles in transcriptional control and RNA processing. *J. Cell. Biochem. 102*, 136–148.
26. Sekimata, M., and Homma, Y. (2004) Sequence-specific transcriptional repression by an MBD2-interacting zinc finger protein MIZF. *Nucleic Acids Res. 32*, 590–597.

27. Huntley, S., Baggott, D. M., Hamilton, A. T., Tran.Gyamfi, M., Yang, S., Kim, J., Gordon, L., Branscomb, E., and Stubbs, L. (2006) A comprehensive catalog of human KRAB-associated zinc finger genes: Insights into the evolutionary history of a large family of transcriptional repressors. *Genome Res. 16*, 669–677.
28. Bardwell, V. J., and Treisman, R. (1994) The POZ domain: A conserved protein-protein interaction motif. *Genes Dev. 8*, 1664–1677.
29. Bellefroid, E. J., Poncelet, D. A., Lecocq, P. J., Revelant, O., and Martial, J. A. (1991) The evolutionarily conserved Kruppel-associated box domain defines a subfamily of eukaryotic multi-fingered proteins. *Proc. Natl. Acad. Sci. U.S.A. 88*, 3608–3612.
30. Williams, A. J., Khachigian, L. M., Shows, T., and Collins, T. (1995) Isolation and characterization of a novel zinc-finger protein with transcription repressor activity. *J. Biol. Chem. 270*, 22143–22152.
31. Grimes, H. L., Chan, T. O., Zweidler.McKay, P. A., Tong, B., and Tsichlis, P. N. (1996) The Gfi-1 proto-oncoprotein contains a novel transcriptional repressor domain, SNAG, and inhibits G1 arrest induced by interleukin-2 withdrawal. *Mol. Cell. Biol. 16*, 6263–6272.
32. Sambrook, J., and Russell, D. W. (2001) *Molecular Cloning: A Laboratory Manual*, Cold Spring Harbor Laboratory Press, Plainview, NY.
33. McLean, R. A., Sanders, W. L., and Stroup, W. W. (1991) A unified approach to mixed linear models. *Am. Stat. 45*, 54–64.
34. Corbeil, R. R., and Searle, S. R. (1976) Restricted maximum likelihood (REML) estimation of variance components in the mixed model. *Technometrics 18*, 31–38.
35. SAS Institute Inc. (1997) *The MIXED Procedure. SAS/STAT Software: Changes and Enhancements through Release 6.12*, SAS Institute, Inc., Cary, NC.
36. Hsu, J. C. (1992) The factor analytic approach to simultaneous inference in the general linear model. *J. Comput. Graphical Stat. 1*, 168.
37. Daniel, W. W. (1990) *Applied Nonparametric Statistics*, Duxbury Press, Pacific Grove, CA.
38. SAS Institute Inc. (2006) *Base SAS 9.1.3 Procedures Guide*, SAS Institute Inc., Gary, NC.
39. Nicholas, K. B., Nicholas, H. B., Jr., and Deerfield, D. W. (1997) GeneDoc: Analysis and visualization of genetic variation. *EMBNEW NEWS 4*, 14.
40. Bennett-Lovsey, R. M., Herbert, A. D., Sternberg, M. J., and Kelley, L. A. (2008) Exploring the extremes of sequence/structure space with ensemble fold recognition in the program Phyre. *Proteins 70*, 611–625.
41. Kelley, L. A., MacCallum, R. M., and Sternberg, M. J. (2000) Enhanced genome annotation using structural profiles in the program 3D-PSSM. *J. Mol. Biol. 299*, 499–520.
42. Collins, T., Stone, J. R., and Williams, A. J. (2001) All in the family: The BTB/POZ, KRAB, and SCAN domains. *Mol. Cell. Biol. 21*, 3609–3615.

BI800961D